ADVANCES IN MATERIALS SCIENCE, Vol. 19, No. 4 (62), December 2019

DOI: 10.2478/adms-2019-0018

L. Łatka[1*], M. Michalak[1], E. Jonda[2]

[1] *Wrocław University of Science and Technology, Mechanical Engineering Faculty, 5 Łukasiewicza St., 50-371 Wrocław, Poland*

[2] *Silesian University of Technology, Mechanical Engineering Faculty, 18a Konarskiego St., 44-100 Gliwice, Poland*

* *leszek.latka@pwr.edu.pl*

ATMOSPHERIC PLASMA SPRAYING OF Al_2O_3 + 13% TiO_2 COATINGS USING EXTERNAL AND INTERNAL INJECTION SYSTEM

ABSTRACT

The ceramic coatings based on mixture of Al_2O_3 and TiO_2 have better properties in comparison to the pure alumina ones. Among many techniques, plasma spraying is very useful method of ceramic coatings manufacturing. In this paper, the results of microscopic, mechanical and tribological properties investigations of Al_2O_3 + 13 wt% TiO_2 coatings manufactured by atmospheric plasma spraying are presented. The cylinder substrates made from stainless steel (X5CrNi18-10) had a diameter equal to 25 mm and thickness equal to 2 mm. The plasma spray experimental parameters included three variables: (i) type of injection system (external or internal), (ii) size of corundum particles for sandblasting and (iii) torch linear speed. The results confirm, that type of injection system is a dominant parameter. Internal injection results in better degree of particles melting, what influences on wear resistance performance, as well as higher values of bond strength.

Keywords: *atmospheric plasma spraying, Al_2O_3 + TiO_2 coating, microstructure, mechanical properties, injection system*

INTRODUCTION

In many cases, the life-time of the elements is related to its surface. A relevant area in the field of surface engineering is thermal spraying. This branch develops very dynamically since 40 years and it is a result of improving techniques, equipment and understanding the processes [1-4]. In thermal spraying coatings are manufactured by introducing feedstock material into a flame [5], arc [6] or plasma jet [7] and then are melted of only heat and accelerated towards the substrate. The coatings growth is continuously layer by layer. The most wide used methods are: high velocity oxy fuel (HVOF), arc wire spraying, cold gas spraying and plasma spraying [8]. Because of many advantages, like good adhesion strength, high deposition rate and high temperature of the jet, plasma spraying is commonly used in different branches of industry, e.g. power generation, general industry, biomedical and abrasive wear applications [9-11]. Moreover, plasma spraying allows using functionally graded materials to produce special coatings [12]. Ceramic coatings manufactured by thermal

spraying are used in wide range of the industrial applications. Presented in this article, Al_2O_3 with TiO_2 materials combination, is used in textile industry tools or in butterfly valves in hydraulic systems [13-16]. Those oxides have relatively high melting temperatures and low thermal conductivities in comparison with metals. Powders consisting of Al_2O_3 with TiO_2 are easier to melt completely because the melting temperature is substantially lower [16]. Therefore, coatings with addition TiO_2 are widely produced – moreover, its presence enhances the mechanical properties and wear resistance of the coatings [15, 17-20].

In this study, Al_2O_3 + 13 wt% TiO_2 coatings were prepared by atmospheric plasma spraying (APS) of micrometer-sized agglomerated and sintered powders. In thermal spraying, the properties of coatings strongly depend on operational conditions. Therefore, in this work, the influence of substrate sandblasting, type of injection and torch scan speed were investigated. The coatings were characterized in the terms of their morphology, microstructure, phase composition and relevant mechanical properties.

MATERIALS AND METHODS

As a coating material, a commercially available powder Metco 6221 (Oerlikon Metco, Germany) was used. The chemical composition of the feeding material is Al_2O_3 + 13 wt% TiO_2. The powder is agglomerated and sintered and its morphology is spheroidal (Fig. 1). The volume-surface mean diameter of the coarse powder was measured to be equal to d_{VS} = 33 μm. The particle size distribution was in the range – 45 + 15 μm.

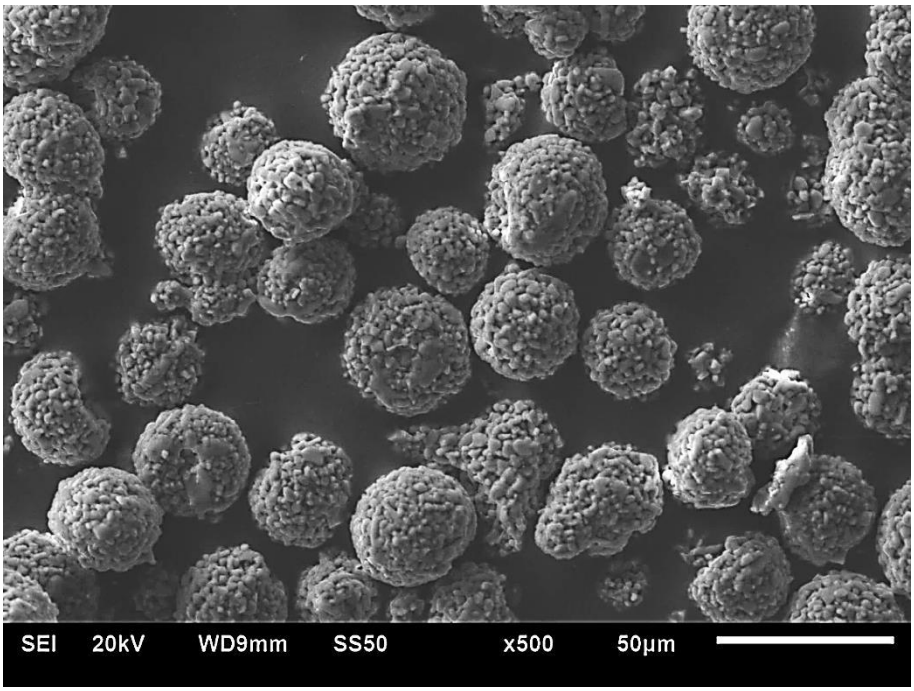

Fig. 1. SEM image of Al_2O_3 + 13 wt% TiO_2 powder in the delivery condition

Atmospheric plasma spraying (APS) method was used to deposit ceramic coatings. The main part of the set-up was SG-100 plasma torch, which was mounted on the arm of the industrial 6-axis Fanuc 2000 IA robot. The powder was introduced into the plasma jet radially and the feed rate was kept constant on the level about 20 g/min. Before spraying the powder

was dried at the temperature of 120 °C for 2 hours, in order to avoid clogging during powder feeding. Plasma spraying was carried out with constant parameters, which are collected in Table 1, while the samples code and variable parameters are given in Table 2.

***Table** 1. Constant process parameters*

Electrical power kW	Primary gas flow rate slpm	Secondary gas flow rate slpm	Transport gas flow rate slpm	Spray distance mm
35	Ar = 45	H_2 = 5	Ar = 3	80

* slmp – standard litre per minute

Austenitic stainless steel (X5CrNi18-10) coupons with a diameter equal to 25 mm and 2 mm in thickness were used as substrates. Before spraying, its surface was sand-blasted by using different corundum grit. After this, the substrates were cleaned with ethanol in the ultrasonic bath.

Coatings' free surfaces and cross-sections were observed by using Phenom G2 Pro (Phenom-World, the Netherlands). Based on those images, the porosity of coatings was evaluated according to ASTM E2109-01 standard, with the use of ImageJ open-source software. The porosity was assessed at 1000x magnification.

The phase composition of the initial powders and coatings was determined by powder X-ray diffraction technique (XRD) using D8 Discover diffractometer (Bruker AXS, Germany) with CuKα radiation. The measurements were performed in the range 2Θ=10°÷80°, with 0.05° step size and 0.8 s/step counting time. The percentage of the phases in examined coatings were determined from the method called reference intensity ratio (RIR), described in [21]. This method based on the comparison of the strongest peaks intensities.

***Table 2.** Sample code and variable process parameters*

Sample code	Type of injection system	Size of corundum particles	Torch velocity mm/s
EB300	External	F20	300
EB500	External	F20	500
ES300	External	F40	300
ES500	External	F40	500
IB300	Internal	F20	300
IB500	Internal	F20	500
IS300	Internal	F40	300
IS500	Internal	F40	500

Microhardness of the coatings was measured with Vickers penetrator under the load of 1.96 N (HV0.2) on the Sinowon HV-1000 apparatus (Sinowon Innovation Metrology, China), according to the PN-EN ISO 4516:2004 standard. 10 imprints in random places of the coating

were made for each sample. After measurements, the average values and standard deviations were calculated.

Fracture toughness *Kc* was determined according to the PN-EN ISO 14577-4:2017-02 standard. The measurements were carried out on the cross-section of the coating. Determination of *Kc* was based on measurement of cracks length, occurred after Vickers penetration. Type of cracks is dependent on material and applied load. Two types are usually distinguished: (i) Palmqvist's – for lower loads and (ii) radial – for higher loads [22]. The details of the methodology are given in paper [23].

The adhesion strength of the coatings was measured in the pull-off test, being carried out according to the PN-EN ISO 14916:2017-05 standard. The samples were prepared with Distal Classic adhesive of medium strength equal to 50 MPa.

Tribological tests were carried out with using of ball-on-disc T-01 tribometer (Rtec instruments, USA) in technically dry friction conditions, according to the ASTM G99 standard. As a counter-part 6mm diameter sintered Al_2O_3 balls were used. Sliding was performed under ambient conditions over of period of 1000 m at sliding velocity of 0.1 m/s and the normal load of 10 N. Four replicate wear tests were carried out and the average results were reported. The worn surfaces of the coatings were observed on a scanning electron microscope (SEM) Phenom G2 PRO. Traces of wear were determined using a contact profilometer (Surtronic 25, Taylor Hobson) and the volumetric wear of the tested coatings was determined by the length of friction path and applied load.

RESULTS AND DISCUSSION

Surfaces of the sprayed coatings are shown in Fig. 2. As it could be seen, the internal injection mode results in topography with well-molten splats (Fig. 2b and 2d). It is caused by longer heat treatment of powder particles in the plasma jet. In case of coatings sprayed with external injection mode (Fig. 2a and 2c), it could be seen not fully melted particles or even grains with dimension equal to the initial size of the powder. It probably results of not enough heat flux received from plasma jet. Some cracks, which could be seen on the top surfaces, are caused by heat transfer from plasma jet into the samples during spraying, which formed thermal stresses and finally cracks. On the other hand, the cracks density is not so great, what was confirmed by other examinations.

The coatings cross-sections are presented in Fig. 3. It could be seen, that the coatings are formed with molten lamellas, which built a homogenous structure. There are some cracks, voids and pores, which are typical imperfections for APS method. On the other hand, for all samples, on the interface between substrate and coating, the roughness asperities are filled with coating material with high quality of adherence. The thickness of all coatings was in the range from 250 to 350 μm. Moreover, the cross-sections observations could provide information about coatings porosity level, which seems to be quite low (generally much below 10%). The results are consistent with the literature [24–26].

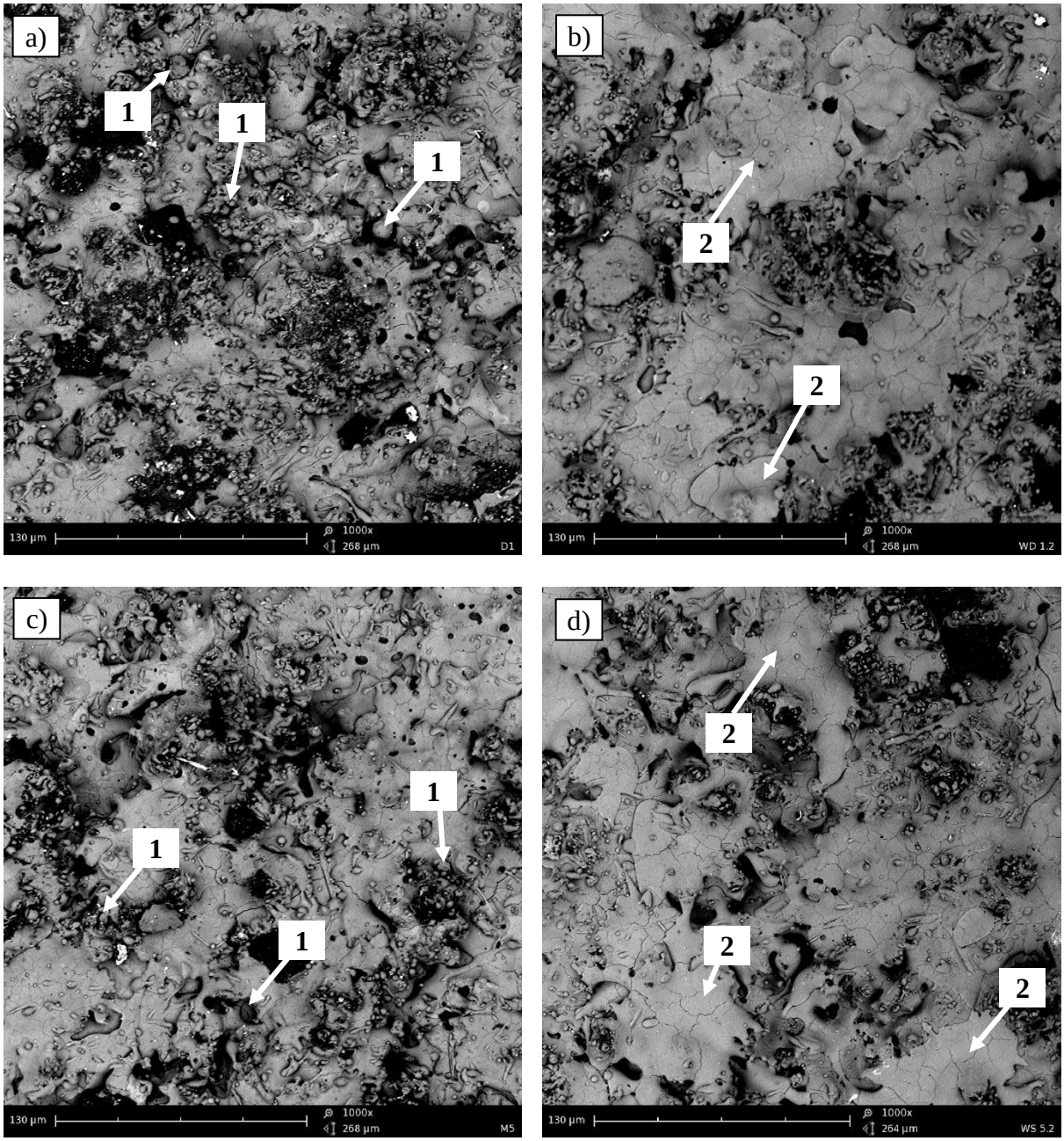

Fig. 2. Coatings topography: (a) EB300, (b) IB300, (c) ES500, (d) IS500, SEM images; 1 – not fully meleted particles, 2 – well melted splats

The phase diagram of the initial powder used in current researches is presented in Fig. 4. It could be seen, that in powder only two phases were detected, namely stable α-Al_2O_3 and anatase TiO_2. Using the RIR method it is possible to determine the phase composition as 80.4% of α-Al_2O_3 and 19.6% of anatase TiO_2. Those phases are mainly identified in the literature in the case of Al_2O_3 + 13 wt% TiO_2 powders [18, 27–29].

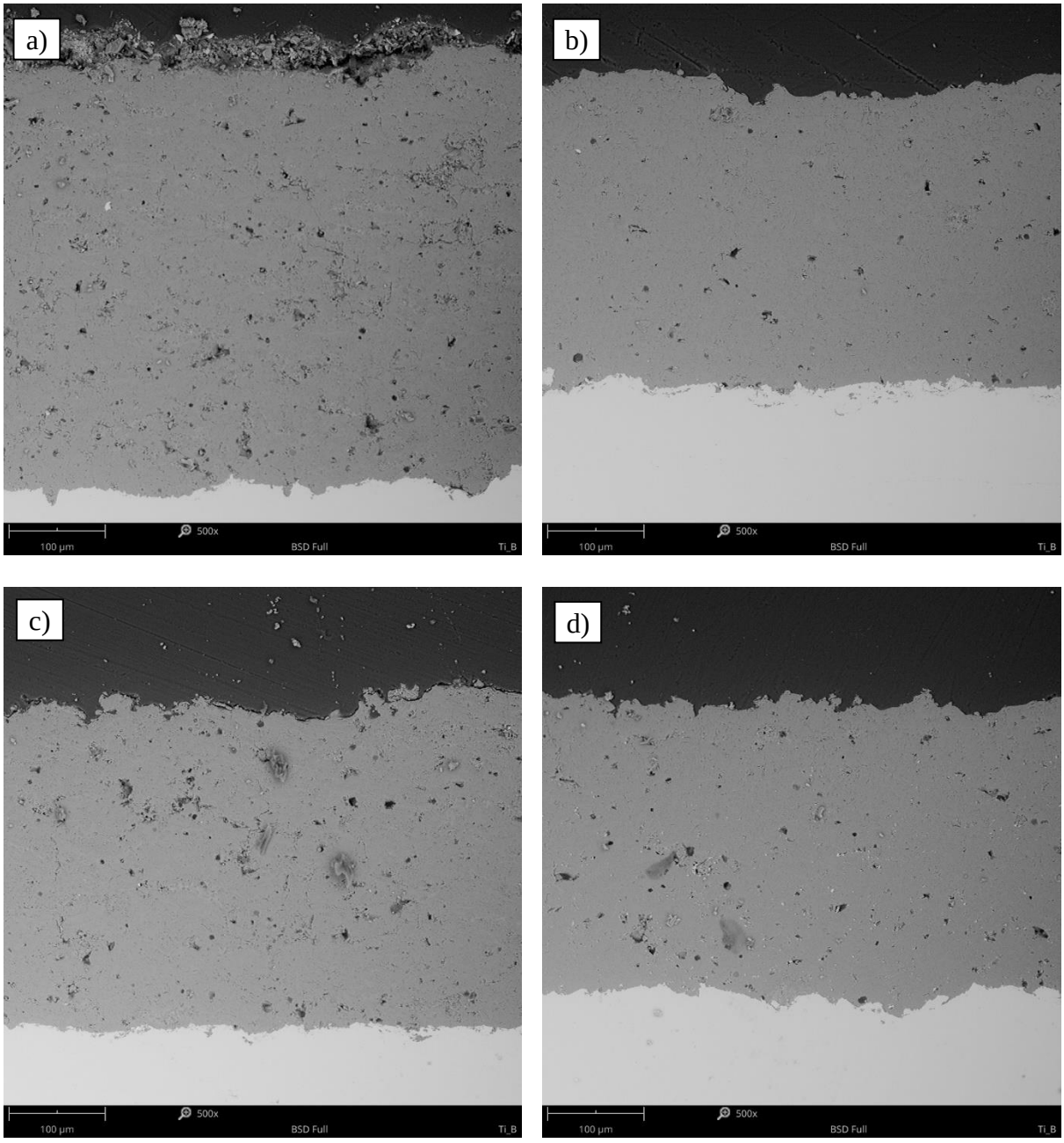

Fig. 3. Coatings cross-section: (a) EB500, (b) IB500, (c) ES300, (d) IS300, SEM

After spraying, the phase composition of the coatings is different, than those of the feedstock material. As it could be seen in Fig. 5, there are four phases: α-Al_2O_3, γ-Al_2O_3, rutile TiO_2 and Al_2TiO_5. These changes are caused by thermal processes, during plasma spraying. From a point of view of good wear resistance, the amount of γ-Al_2O_3 phase should be minimalized. In case of TiO_2, during thermal spraying, the irreversible transformation anatase into rutile occurs. And finally, the Al_2TiO_5 phase appears as a result of mixing two ingredients of initial powder [19,24,27,29–31].

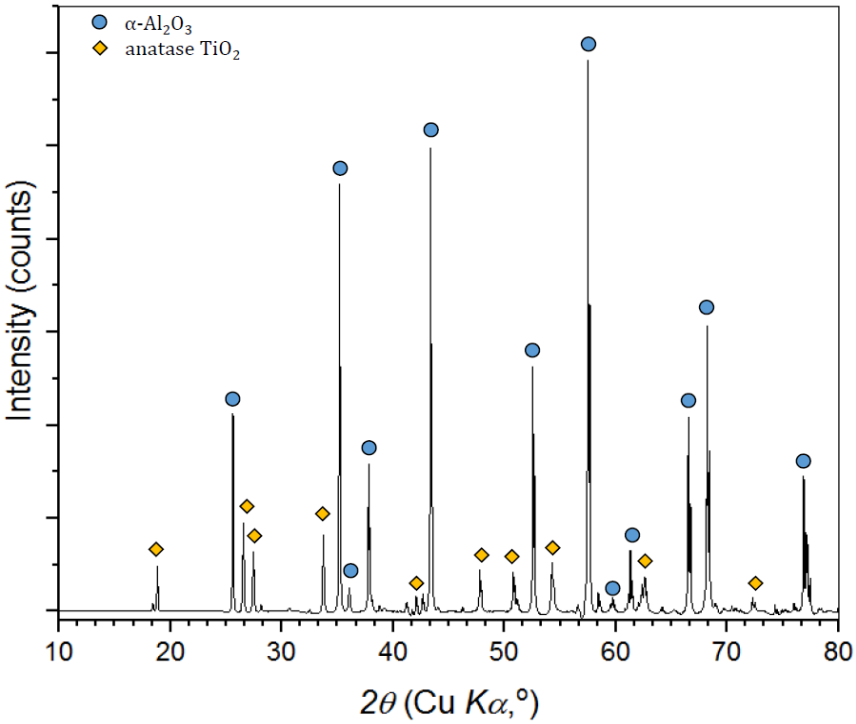

Fig. 4. X-ray diagram of feedstock (powder in delivery condition)

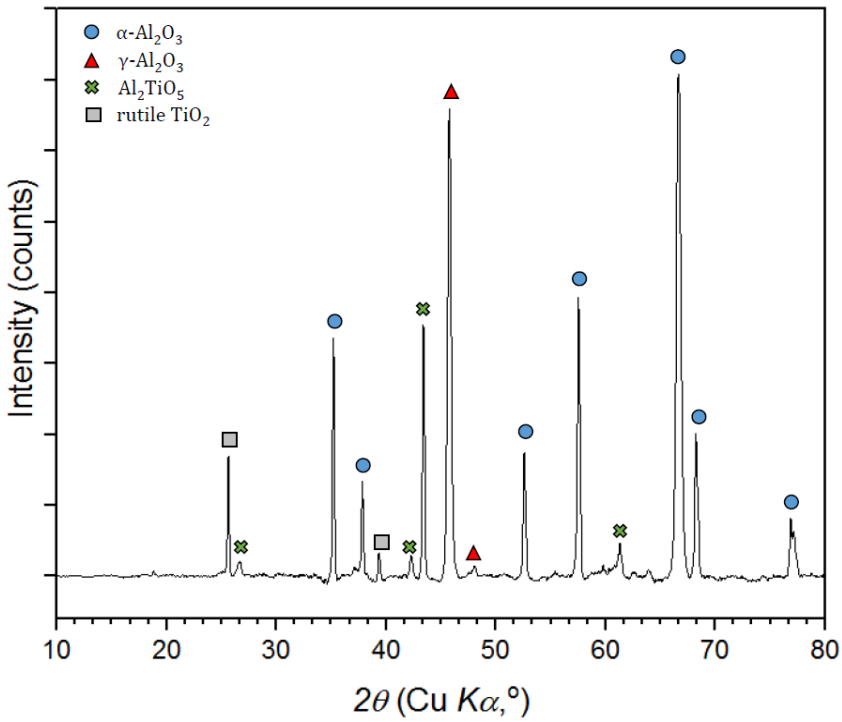

Fig. 5. X-ray diagram of sprayed coating (IB300)

For all coatings the differences in phase composition were not significant. A clear dependence was observed, namely a higher content of α-Al_2O_3 phase in case of coatings manufactured with internal injection mode. The range of phases content is summarized in Table 3.

Table 3. *The range of phases content in coatings manufactured by APS method*

Phases occurring in APS coatings, % content			
α-Al_2O_3	γ-Al_2O_3	rutile TiO_2	Al_2TiO_5
48.7 – 55.2	33.8 – 39.6	7.6 – 11.4	3.4 – 6.7

In Table 4 the mean values of porosity, microhardness and fracture toughness of sprayed coatings are compared. As it could be seen, a correlation between these values exists. Generally, coatings with lower porosity level exhibit higher microhardness, which is connected with more homogenous structure and smaller quantity of material discontinuities. Very low values of standard deviation for porosity confirm that coatings have regular and homogenous structure. On the other hand, in the case of coatings with higher porosity level, the standard deviation of microhardness is also bigger, which is connected with irregular structure. The dependence between microhardness and fracture toughness is observed as well. For samples which exhibit lower microhardness values, the fracture toughness values are bigger. The values of measured hardness and fracture toughness are close to those presented in the literature – Yilmaz et al. [15] obtained Al_2O_3 + 13 wt% TiO_2 coatings with the hardness equal to 853 HV0.2 and fracture toughness 3.7 MPa/m$^{1/2}$. Also Yugesvaran et al. [25] and Jafarzadeh et al. [26] obtained similar results.

Table 4. *Mean values of the porosity, microhardness and fracture toughness of sprayed coatings*

	EB300	EB500	IB300	IB500	ES300	ES500	IS300	IS500
porosity %	6.8 ± 0.2	7.2 ± 0.5	5.0 ± 0.5	3.8 ± 0.4	6.7 ± 0.6	9.3 ± 0.6	3.9 ± 0.4	4.9 ± 0.4
microhardness HV0.2	787 ± 72	762 ± 85	801 ± 77	812 ± 79	773 ± 82	754 ± 98	806 ± 74	793 ± 85
fracture toughness MPa/m$^{1/2}$	3.42 ± 0.23	3.61 ± 0.19	3.44 ± 0.26	3.24 ± 0.21	3.56 ± 0.25	3.72 ± 0.29	3.33 ± 0.18	3.36 ± 0.23

The bonding strength of manufactured coatings was determined in the pull-off test. The results are collected in Fig. 6. The main values are in the range from 17 up to 23 MPa. In general, two dependences could be noticed. One is connected with injection mode. For the internal system, the adhesion was better, which is caused by better heat treatment in the plasma jet. Another correlations show, that coatings, which were sprayed onto the substrates, which had higher roughness (bigger corundum particles, F20) exhibit better adhesion. Similar results are obtained in [18, 20, 32]. What is very important, all values are higher, than industrial requirements (min. 15 MPa) for this type of coatings. The influence of torch scan speed is negligible when comparing with injection mode and size of corundum.

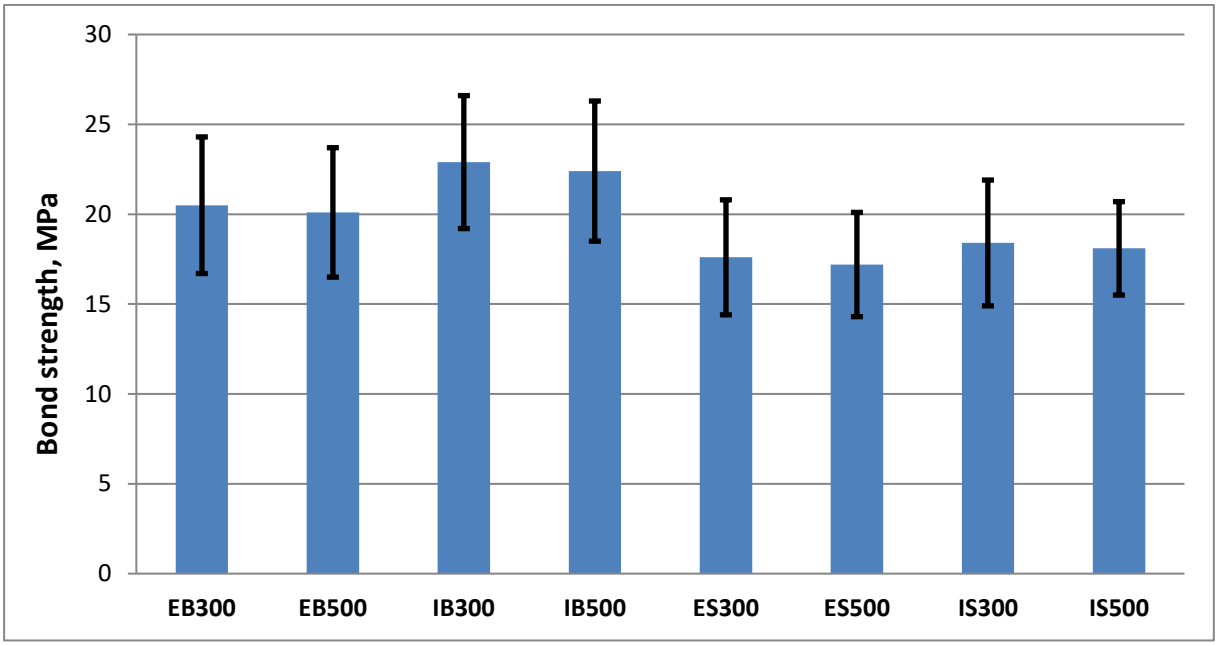

Fig. 6. Bond strength of manufactured coatings

Volume wear rates of investigated coatings are presented in Fig. 7. Wear is a very complex process and many factors, including microhardness, fracture toughness, microstructure, influence on it. As could be seen in the presented study, toughness the most significantly determines the wear resistance of the coating. It could be observed that EB500 and ES500 samples (with the highest values of fracture toughness) have the highest volume wear values. These results are consistent with the studies of other authors [20]. Good wear resistance is connected with well-molten lamellas and good adhesion between them. Moreover, lower porosity is also promoted to exhibit good wear resistance [33]. Results show also that the increased speed of the torch provides coatings with lower wear rate.

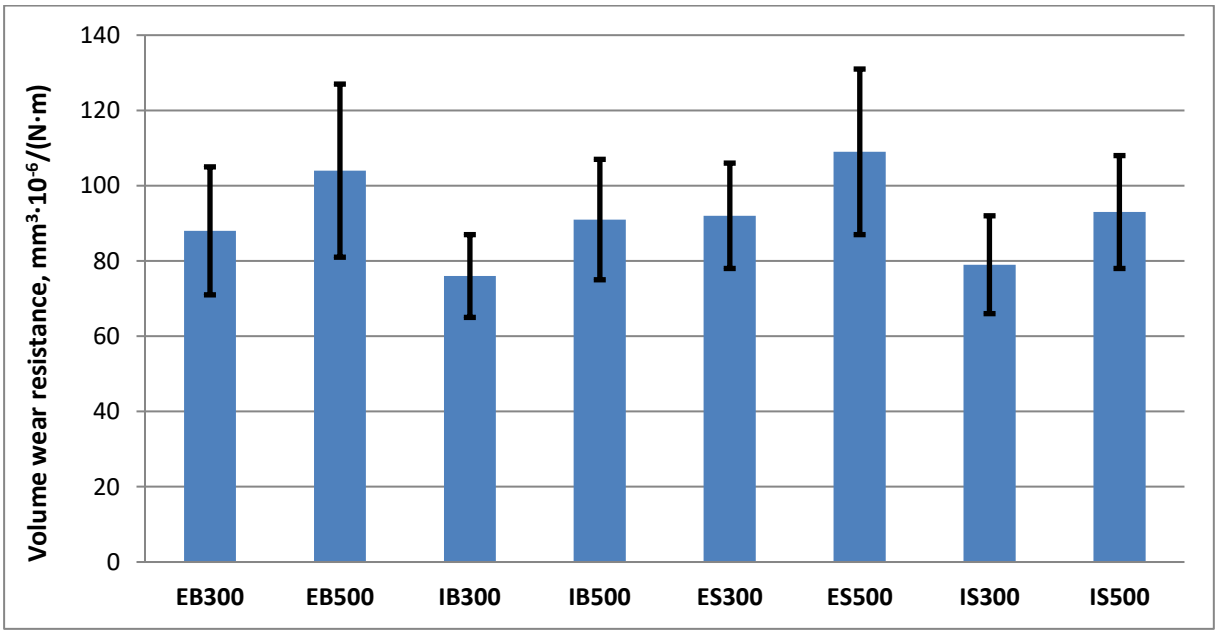

Fig. 7. Volume wear resistance of manufactured coatings

SEM investigations of wear tracks (Fig. 8) show the existence of uniform surface after wear, with visible grooves. Nevertheless, its morphology is different for internal (Fig. 8a) and external (Fig. 8b) injection. It may be related to the fact that internally-injected coating was built of well-molten splats, on the contrary to the coating produced by external injection, with a lot of non-fully melted particles. Those particles could be detached easily. Next, not all of them were removed from the contact area, and some of them enter the ball surface, being initially crushed, rolled and then pressed into the friction track. The result is a local strengthening of the material and a "pseudo-composite" structure, consisting of an exposed coating and dispersed hard products ball material – and finally, higher wear resistance [33, 34]. Moreover, it is clearly visible the difference between wide of the wear tracks in case of IB300 (Fig. 8a) and ES500 (Fig. 8b) samples, which is also connected with resistance against wear.

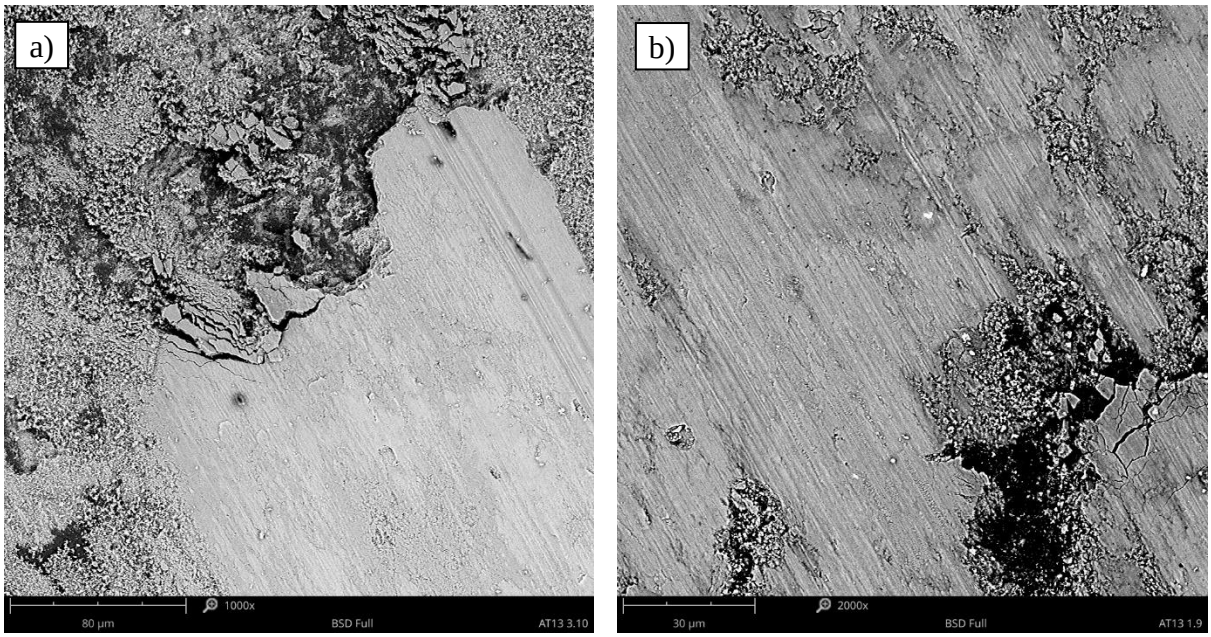

Fig. 8. Wear tracks of sprayed coatings: (a) IB300 and (b) ES500

CONCLUSIONS

In presented paper different process variables (powder injection mode, size of corundum particles used in substrate preparation and velocity of plasma torch) were used in order to manufacture Al_2O_3 + 13wt% TiO_2 coatings by APS method. The aim of these researches was to describe the effect of above mentioned parameters on the deposition process. Afterwards, sprayed samples were characterized in terms of its microstructure and various mechanical properties. The results of carried out researches lead to making the following conclusions:

- the main influence on the coatings microstructure and mechanical properties exhibits the type of powder injection;
- coatings obtained with internal injection mode show a more compact structure with a greater number of fully molten particles, which is a result of longer heat treatment in plasma jet;

- furthermore, with internal injection deposited coatings were more homogenous and were characterized by higher microhardness (about 10%) and lower porosity level (almost 2 times) in compare to coatings sprayed with external powder injection;
- the good wear resistance observed for coatings series IB and IS is connected with an increase in the α-Al_2O_3 phase content because of desirable retention of this phase in the coatings without any post-treatment;
- better cohesion in the IB and IS coatings is a result of improved particles heat treatment in the plasma jet, what is strongly connected with superior wear resistance characteristic;
- the bonding strength is strongly connected with injection mode and with type of substrate preparation, which was realized by different corundum particles size (F20 and F40), in case of injection mode coatings series IB and IS have better adhesion (about 10%) than coatings series EB and ES;
- in case on corundum particles size, using F20 results in formation of higher roughness, which was more suitable for powder particles and finally results in better adhesion (about 15%) than in case of F40;
- spraying parameters such as torch scan speed influenced especially the volume wear rate of the coatings – higher speed resulted in higher wear resistance of the deposits;
- the substrate roughness should be correlate with initial powder particles size.

The future studies will focus on the influence of the spray distance, as well as the plasma enthalpy (type and flow rate of plasma gases) on the manufactured coatings and its mechanical properties.

ACKNOWLEDGEMENTS

These researches were funded by Ministry of Science and Higher Education, grant number 4283/E-366/M/2018

REFERENCES

1. Fauchais P., Vardelle A.M., Dussoubs B., Quo Vadis Thermal Spraying? Journal of Thermal Spray Technology, 2001, Vol. 10(1), 44–66.
2. Szala M., Hejwowski T., Cavitation erosion resistance and wear mechanism model of flame-sprayed Al_2O_3-40% TiO_2/NiMoAl cermet coatings, Coatings, 8 (2018) 254.
3. Czupryński A., Selected properties of thermally sprayed oxide ceramic coatings, Advances in Materials Science, 15 (2015) 17–32.
4. Łatka L., Thermal barrier coatings manufactured by suspension plasma spraying – a review, Advances in Materials Science, 18 (2018) 95–117.
5. Musztyfaga-Staszuk M., Czupryński A., Kciuk M., Investigation of mechanical and anti-corrosion properties of flame sprayed coatings, Advances in Materials Science, 18 (2018) 42–53.
6. Chmielewski T., Siwek P., Chmielewski M., Piątkowska A., Grabias A., Golański D., Structure and selcted properties of arc sprayed coatings containing in-situ fabricated Fe-Al intermetallic phases, Metals, 8 (2018) 1059.
7. Wypych A., Siwak P., Andrzejewski D., Jakubowicz J., Titanium plasma-sprayed coatings on polymers for hard tissue applications, Materials, 11 (2018) 2536.

8. Winnicki M., Baszczuk A., Jasiorski M., Małachowska A., Corrosion resistance of cooper coatings deposited by cold spraying, Journal of Thermal Spray Technology, 26 (2017) 1935-1946.
9. Pawłowski L., The Science and Engineering of Thermal Spray Coatings, 2nd. ed. , Wiley, Chichester, U.K., 2008.
10. Candidato R.T., Sokołowski P., Łatka L., Kozerski S., Pawłowski L., Denoirjean A., Plasma spraying of hydroxyapatite coatings using powders, suspension and solution feedstock, Przegląd Spawalnictwa, 87 (2015) 64-71.
11. Szala M., Dudek A., Maruszczyk A., Walczak M., Chmiel J., Kowal M., Effect of atmospheric plasma sprayed TiO2-10% NiAl cermet coatings thickness on cavitation erosion, sliding and abrasive wear resistance, Acta Physica Polonica A, 136 (2019) 335-341.
12. Basu B., Balani K.: Advanced Structural Ceramics, Basu B. [ed.], John Wiley & Sons, New Jersey, 2011.
13. Toma F.-L., Berger L.-M., Stahr C.C., Naumann T., Langner S., Microstructures and functional properties of suspension-sprayed Al2O3 and TiO2 coatings: an overview, Journal of Thermal Spray Technology, 19(1–2) (2010) 262-274.
14. Berger L.-M., Sempf K., Sohn Y.J., Vassen R., Influence of Feedstock Powder Modification by Heat Treatments on the Properties of APS-Sprayed Al2O3-40% TiO2 Coatings, Journal of Thermal Spray Technology, 27(4) (2018) 654–666.
15. Yilmaz R., Kurt A.O., Demir A., Tatli Z., Effects of TiO_2 on the mechanical properties of the Al_2O_3-TiO_2 plasma sprayed coating, Journal of the European Ceramic Society, 27 (2007) 1319–1323.
16. Sanchez E., Bannier E., Cantavella V., Salvador M.D., Klyatskina E., Morgiel J., Grzonka J., Boccaccini A.R., Deposition of Al_2O_3-TiO_2 Nanostructured Powders by Atmospheric Plasma Spraying, Journal of Thermal Spray Technology, 17 (2008) 329–337.
17. Kroemmer M.: Practice of thermal spraying: Guidance for technical personnel, Kroemmer M. [ed.], DVS Media GmbH, Hagen, 2014.
18. Dejang N., Watcharapasorn A., Wirojupatump S., Niranatlumpong P., Jiansirisomboon S., Fabrication and properties of plasma-sprayed Al_2O_3/TiO_2 composite coatings: A role of nano-sized TiO_2 addition, Surface and Coatings Technology, 2014 (2010) 1651–1657.
19. Mishra S.C., Sahu A.: Alumina-Titania Overlay Coating on Metals: Surface Modification, Mishra S.C. [ed.], LAP LAMBERT Academic Publishing, 2017.
20. Zhang J., He J., Dong Y., Li X., Yan D., Microstructure and properties of Al_2O_3-13%TiO_2 coatings sprayed using nanostructured powders, Rare Metals, 26 (2007) 391–397.
21. Prevey P.S., X-ray diffraction characterization of crystallinity and phase composition in plasma-sprayed hydroxyapatite coatings, Journal of Thermal Spray Technology, 9 (2000) 369-376.
22. Palmqvist S., Occurrence of crack formation during Vickers indentation as a measure of the toughness of hard metals, Archiv für das Eisenhüttenwesen, 33 (1962) 629–633.
23. Michalak M., Łatka L., Sokołowski P., Porównanie właściwości mechanicznych powłok natryskiwanych plazmowo proszkowo i z zawiesin, Przegląd Spawalnictwa 10 (2017) 56–60.
24. Vincent M., Bannier E., Moreno R., Salvador M.D., Sanchez E., Atmospheric plasma spraying coatings from alumina-titania feedstock comprising bimodal particle size distribution, Journal of European Ceramic Society, 33 (2013) 3313–3324.
25. Yugeswaran S., Selvarajan V., Vijay M., Ananthapadmanabhan P.V. , Sreekumar K.P.: Influence of critical plasma spraying parameter (CPSP) on plasma sprayed Alumina–Titania composite coatings, Ceramics International, 36 (2010) 141–149.

26. Jafarzadeh K., Valefi Z., Ghavidel B., The effect of plasma spray parameters on the cavitation erosion of Al_2O_3–TiO_2 coatings, Surface and Coatings Technology, 205 (2010) 1850–1855.
27. Islak S., Buytoz S., Ersoz E., Orhan N., Stokes J., Saleem Hashmi M., Somunkiran I., Tosun N., Effect on microstructure of TiO_2 rate in Al_2O_3-TiO_2 composite coating produced using plasma spray method, Optoelectronics and advanced materials – rapid communications, 6 (2012) 884–849.
28. Stengl V., Ageorges H., Ctibor P., Murafa N., Atmospheric plasma sprayed (APS) coatings of Al_2O_3–TiO_2 system for photocatalytic application, Photochemical & Photobiological Sciences, 8 (2009) 733–738.
29. Yao S.H., Su Y.L., Shu H.Y., Chia L., Ling Y.Z., Comparative Study on Nano-Structural and Traditional Al_2O_3-13TiO_2 Air Plasma Sprayed Coatings and their Thermal Shock Performance, Key Engineering Materials, 739 (2017) 103–107.
30. Vijay M., Selvarajan V., Yugeswaran S., Ananthapadmanabhan P.V., Sreekumar K.P., Effect of Spraying Parameters on Deposition Efficiency and Wear Behavior of Plasma Sprayed Alumina-Titania Composite Coatings, Plasma Science and Technology, 11(2009) 666–673.
31. Lima R.S., Marple B.R., Thermal Spray Coatings Engineered from Nanostructured Ceramic Agglomerated Powders for Structural, Thermal Barrier and Biomedical Applications: A Review, Journal of Thermal Spray Technology, 16 (2007) 40–63.
32. Jordan E.H., Gell M., Sohn Y.H., Goberman D., Shaw L., Jiang S., Wang M., Xiao T.D., Wang Y., Strutt P., Fabrication and evaluation of plasma sprayed nanostructured alumina–titania coatings with superior properties, Materials Science and Engineering, A 301 (2001) 80-89.
33. Żórawski W., Góral A., Makrenek M., Zimowski S., Tribological properties of plasma sprayed Al_2O_3-13TiO_2 nanostructured coatings, Tribologia, 2 (2017) 157-165.
34. Zimowski S., Rakowski W., Comparative analysis of friction effects of thin ceramic coatings in rotary, translation, and reciprocating motion, Tribologia, 6 (2009) 283–292.